ASSESSING SOIL PROPERTIES VIA NIR-VIS SPECTRAL ANALYSIS USING 1D-CNN MODELS WITH INSIGHTS INTO INTERPRETABILITY

HE, P.[1,2,3#] – CHENG, X. F.[4,5#] – WEN, X. P.[1*] – YI, Y.[2] – ZOU, Y.[2] – MAO, Z. F.[2] – CHEN, Z. L.[4,5] – CHEN, Y.[3,6*]

[1]*Faculty of Land Resources Engineering, Kunming University of Science and Technology, Kunming 650093, China*

[2]*School of Fine Art and Design, Kunming University, Kunming 650214, China*

[3]*International Research Center of Big Data for Sustainable Development Goals, Beijing 100094, China*

[4]*School of Earth and Environmental Sciences, Yunnan Land and Resources Vocational College, Kunming 652501, China*

[5]*Engineering Center of Yunnan Education Department for Health Geological Survey & Evaluation, Kunming 650218, China*

[6]*Key Laboratory of Digital Earth Science, Aerospace Information Research Institute, Chinese Academy of Sciences, Beijing 100094, China*

[#]*Ping He and Xianfeng Cheng contributed equally to this study*

**Corresponding authors*
e-mail: wxp@kust.edu.cn; chenyu@radi.ac.cn

(Received 10th Jun 2025; accepted 21st Aug 2025)

Abstract. Soil quality assessment relies on key indicators such as total nitrogen (TN), organic carbon (OC), and pH. Visible and near-infrared (Vis-NIR) spectroscopy, paired with one-dimensional Convolutional Neural Networks (1D-CNNs), offers an effective tool for soil analysis. This study uses the LUCAS dataset to evaluate 1D-CNN architectures (1D-LeNet, 1D-AlexNet, 1D-VGG, 1D-ResNet), Partial Least Squares (PLS), and Support Vector Machine (SVM) models for predicting TN, OC, and pH. The 1D-LeNet model delivered optimal results, with R^2 scores of 0.92 for TN, 0.95 for OC, and 0.89 for pH. Most 1D-CNNs outperformed PLS and SVM, except 1D-AlexNet, which showed lower precision in pH prediction. SHapley Additive exPlanations (SHAP) value analysis revealed the contribution of specific wavelength bands to predictions, highlighting how different 1D-CNN architectures capture unique soil features. These findings validate the scalability of deep learning for soil spectroscopy and demonstrate its potential to support precision agriculture through fast nutrient monitoring and the development of satellite-based sensing systems.
Keywords: *1D-CNN models, interpretability analysis, total nitrogen, organic carbon, pH*

Introduction

Soil constitutes the foundation of agricultural production, with chemical components like TN, OC, and pH being essential for healthy crop development and yields (Huang et al., 2007). The precise and swift determination of these soil components is crucial for optimizing agricultural practices and strategic decision-making (Islam et al., 2003). Traditional methods for detecting soil components, such as chemical analysis, are precise

http://www.aloki.hu ● ISSN 1589 1623 (Print) ● ISSN 1785 0037 (Online)
DOI: http://dx.doi.org/10.15666/aeer/2306_1073510749
© 2025, ALÖKI Kft., Budapest, Hungary

but often slow and costly (Marcos et al., 2006). Consequently, there is an urgent need for more efficient and precise approaches to evaluate soil components, a subject that has attracted considerable interest in current studies (Kawamura et al., 2021; Seema et al., 2020).

Progress in spectroscopic methods has enabled easier access to Vis-NIR spectral data for soils, opening new opportunities to estimate soil properties (Omondiagbe et al., 2024). Traditional modeling approaches, like PLS and SVM, have seen extensive use in analyzing spectral data related to soil (Allo et al., 2020). Yet, these approaches often face challenges in processing complex, multidimensional, and nonlinear datasets, restricting their capacity to fully utilize spectral information.

With the surge in deep learning technologies, particularly CNNs, there is significant potential to process complex data, driven by their strong feature extraction capabilities and ability to model nonlinear relationships (Meng et al., 2024; Shen et al., 2022). Current research primarily focuses on two main areas. The first is the improvement of classic CNN frameworks. Tsakiridis et al. (2020) presented a localized 1D-CNN framework featuring multiple channels to estimate ten soil attributes, drawing on the LUCAS dataset. Similarly, Zhong et al. (2021) utilized ResNet-16 and VGGNet-16 architectures to model seven soil traits, drawing on LUCAS data. The second area explores the combination of different models and CNN architectures to enhance prediction performance. Ke et al. (2024) incorporated an encoder-decoder structure into the 1D-CNN framework to enhance model accuracy, while Yang et al. (2020) combined CNN and RNN structures to estimate soil properties using LUCAS data. Although substantial research has compared various deep learning models or developed new models (Gruszczyński et al., 2022; Piccoli et al., 2023; Tsimpouris et al., 2021), systematic studies comparing classic CNN architectures of different depths to identify the most accurate 1D-CNN model are limited. Furthermore, while deep learning models demonstrate excellent predictive performance, their “black box” nature restricts model interpretability and practical application. To address this, some studies have utilized SHAP values to elucidate the model decision-making process (Chen et al., 2022; Zhong et al., 2024). SHAP analysis enables evaluation of whether key wavelength bands align with the spectral response characteristics of soil components, thereby validating model rationale and scalability while offering a scientific foundation for future spectral data collection and satellite sensor design. However, further research is needed to determine whether SHAP values can effectively reveal accuracy differences among models, particularly the relationship between high-contribution bands and soil component correlations.

This study aims to evaluate the predictive power of different 1D-CNN architectures for key soil properties. We selected four classical 1D-CNN architectures—1D-LeNet, 1D-AlexNet, 1D-VGG, and 1D-ResNet—to predict soil TN, OC, and pH. Additionally, we further compared the performance of these deep learning models with traditional PLS and SVM models to comprehensively provide the relative advantages of the former in predictions of soil components. The SHAP value analysis method was employed to enhance interpretability by uncovering how 1D-CNN models make predictions. SHAP analysis enabled the identification of the regions of wavelength that contributed most to each one of these predictions in the various bands and provided insight into how best to optimize acquisition and data processing of soil spectral data, enhancing model transparency and operability.

http://www.aloki.hu ● ISSN 1589 1623 (Print) ● ISSN 1785 0037 (Online)
DOI: http://dx.doi.org/10.15666/aeer/2306_1073510749
© 2025, ALÖKI Kft., Budapest, Hungary

Materials and methods

Soil dataset

This research capitalized on the LUCAS dataset, a comprehensive collection managed by the European Soil Data Center. This dataset encompasses 19,036 soil samples gathered from diverse ecological regions across the EU, reflecting a broad spectrum of climatic conditions, topographical features, and land utilization categories (Stevens et al., 2013). The LUCAS dataset was acquired using systematic sampling on a priori defined network points with a nominal interval of about 2 km. From every sampling location, topsoil was sampled for further analysis (Orgiazzi et al., 2017). In the laboratory, these samples underwent spectroscopic analysis using the FOSS XDS Rapid Content Analyzer (FOSS NIRSystems Inc., Denmark) (Orgiazzi et al., 2017). Spectral measurements were taken across the 350-2500 nm range with 2 nm intervals, and after resampling at 0.5 nm intervals, the data yielded a 4200-dimensional dataset (Rinnan et al., 2009).

Model selection and evaluation

CNN models

CNN started gaining more innovations since its first proposal in the late 1980s. One of the early CNN architectures, LeNet-5, was introduced by Yann LeCun and colleagues in 1998. It integrates multiple convolutional and pooling layers, employing local connections and shared weights to minimize parameters while boosting computational efficiency (Lecun et al., 1998). With increasing computation capability and available large-scale data, more and more complex architectures of CNN have been emerging. In 2012, AlexNet marked a significant turning point in image classification tasks, as it introduced ReLU activation and Dropout, both of which significantly improved model performance (Krizhevsky et al., 2012). Later, in 2014, the VGG network, proposed by Simonyan and Zisserman, introduced deeper structures by stacking small 3 × 3 convolutional kernels, balancing parameter count and receptive field size (Krichen, 2023). In 2015, He and colleagues introduced the ResNet, incorporating residual blocks to address gradient degradation issues in deep architectures, enabling the training of substantially deeper networks (He et al., 2016).

To evaluate the predictive efficacy of various CNN architectures for soil components, this study modified classical models to develop one-dimensional CNN variants: 1D-LeNet, 1D-AlexNet, 1D-VGG, and 1D-ResNet. The original spectral resolution was resampled from 0.5 to 1 nm across all 1D-CNN models, reducing the input dimension from 4200 to 2100, reducing data volume and computational complexity while minimizing noise. Applying a logarithmic transformation to the spectra, which utilized the logarithm of spectral reflectance (logR) as the input, served to amplify spectral features and enhance data differentiation, thereby potentially boosting model accuracy. The 1D-CNN models varied in complexity, with filter counts ranging from 6 to 512, kernel sizes from 3 to 11, and strides up to 4 to reduce spatial dimensions, as detailed in *Table 1*; 1D-AlexNet incorporated Dropout (0.5) to mitigate overfitting, while 1D-ResNet used residual blocks to enhance training stability. Across these 1D-CNN models, the number of convolutional layers varies as 2, 5, 8, and 1; max-pooling layers as 2 (average pooling for 1D-LeNet), 3, 5, and 1; and fully connected layers as 3, 3, 3, and 2, respectively, with 1D-ResNet incorporating eight residual blocks and one global pooling layer (see *Table 1* for detailed configurations). For consistent

http://www.aloki.hu ● ISSN 1589 1623 (Print) ● ISSN 1785 0037 (Online)
DOI: http://dx.doi.org/10.15666/aeer/2306_1073510749
© 2025, ALÖKI Kft., Budapest, Hungary

comparative evaluation, all models employ the ReLU activation function across convolutional and output layers.

Training of these models was conducted using the Adam optimizer, targeting a mean squared error (MSE) as the performance metric, over 2000 epochs. A patience parameter of 40 was applied for early stopping, terminating training if validation loss did not improve during the defined epoch window. Implementation of all models was executed in a Python 3.9 environment.

Table 1. *Architectural specifications of various 1D-CNN models*

Layer #	1D-LeNet	1D-AlexNet	1D-VGG	1D-ResNet
In	log(R)	log(R)	log(R)	log(R)
L1	C (6, 5)	C (96, 11, s4)	Conv1D (64, 3)	C (64, 7, s2)
P1	P (2, avg)	P (3, s2)	P (2, s2)	P (3, s2)
L2	C (16, 5)	C (256, 5)	C (128, 3)	2×R (64, 3)
P2	P (2, avg)	P (3, s2)	P (2, s2)	-
L3	-	C (384, 3)	C (256, 3)	R (128, 3, s2)
L4	-	C (384, 3)	C (256, 3)	R (128, 3)
P3	-	-	P (2, s2)	-
L5	-	C (256, 3)	C (512, 3)	R (256, 3, s2)
L6	-	-	C (512, 3)	R (256, 3)
P4	-	P (3, s2)	P (2, s2)	-
L7	-	-	C (512, 3)	R (512, 3, s2)
L8	-	-	C (512, 3)	R (512, 3)
P5	-	-	P (2, s2)	-
G	-	-	-	G (avg)
F	Flatten	Flatten	Flatten	-
FC1	FC (120)	FC (120)	FC (120)	FC (512)
D1	-	D (0.5)	-	-
FC2	FC (84)	FC (84)	FC (84)	-
D2	-	D (0.5)	-	-
Out	FC (1)	FC (1)	FC (1)	FC (1)

In: Input; L#: Conv layer (filters, kernel size, stride); P#: Pooling (size, type/stride); G: Global Pooling (type); F: Flattening; FC#: Fully Connected (units); D#: Dropout (rate); Out: Output; C: Conv1D; P: Pooling (avg for average); R: ResidualBlock; s: stride

PLS and SVM models

PLS models function by detecting underlying factors that enhance the connection linking input features and their responses (Wu et al., 2005). SVM are advanced supervised learning models designed to create hyperplanes useful for classification or regression tasks (Kok et al., 2021). This study constructed models for soil variables TN, OC, and pH: PLS-N, PLS-OC, PLS-pH, SVM-N, SVM-OC, SVM-pH to evaluate the efficacy of 1D-CNN models against PLS and SVM. The optimal component count for PLS was identified through cross-validation paired with a grid search, yielding 41 for PLS-N, 27 for PLS-OC, and 47 for PLS-pH. Bayesian optimization was employed to identify the

http://www.aloki.hu ● ISSN 1589 1623 (Print) ● ISSN 1785 0037 (Online)
DOI: http://dx.doi.org/10.15666/aeer/2306_1073510749
© 2025, ALÖKI Kft., Budapest, Hungary

most advantageous settings for SVM models: (1) SVM-N with C = 0.14, gamma = "auto," and a "linear" kernel; (2) SVM-OC with C = 7.77, gamma = "scale," and an "rbf" kernel; (3) SVM-pH with C = 12.18, gamma = "scale," and an "rbf" kernel. Implementation of both PLS and SVM models utilized the Sklearn library within a Python 3.9 environment.

Data splitting and evaluation metrics

The dataset, consisting of 19,036 samples, was partitioned into a training subset (75%, or 14,277 samples) and a test subset (25%, or 4759 samples). To reduce potential bias from a single random split, the data was randomly divided into these subsets 10 times. Final evaluation indicators, including coefficient of determination (R^2), root mean square error (RMSE), and ratio of performance to deviation (RPD), were derived from mean results across these 10 independent runs. R^2 indicates the model's explanatory power, RMSE measures the size of the prediction error, and RPD assesses predictive accuracy. A well-performing model typically achieves higher R^2 and RPD values, along with a lower RMSE (Liu et al., 2023).

Interpretability

SHAP is a technique rooted in game theory that assigns model predictions to specific feature values for explanation (Albinet et al., 2022). SHAP values have been assigned for each wavelength in the prediction, after which the detection of some key spectral regions is enabled (Zhong et al., 2024). This provides insight into the internal decision-making by the model in great detail and hence carries higher transparency and interpretability. We first trained 1D-CNN models on target variables to ensure their experiment was accurate. Then, 600 randomly picked samples from the training set were used as background data to estimate a baseline, which was later used to calculate the SHAP values. Using the Gradient-based method, SHAP values of 100 randomly chosen test samples are calculated.

Results

Prediction results of different 1D-CNN architectures

In this study, we utilized 1D-LeNet, 1D-AlexNet, 1D-VGG, and 1D-ResNet architectures to predict soil components such as TN, OC, and pH. These models are denoted as 1D-LeNet-N, 1D-AlexNet-N, 1D-VGG-N, 1D-ResNet-N, 1D-LeNet-OC, 1D-AlexNet-OC, 1D-VGG-OC, 1D-ResNet-OC, 1D-LeNet-pH, 1D-AlexNet-pH, 1D-VGG-pH, and 1D-ResNet-pH. Each model was assessed across 10 prediction rounds using the test subset, and scatter diagrams showing observed versus model predictions were generated (*Figs. 1–3*). The results indicate that the 1D-LeNet models consistently outperformed the others in predicting all soil components, while the 1D-AlexNet models performed the worst. Specifically, the metrics R^2, RMSE, and RPD for 1D-LeNet-N stood at 0.92, 1.04, and 6.32, respectively, compared to 0.86, 1.4, and 4.32 for 1D-AlexNet-N. For 1D-LeNet-OC, these values were 0.95, 20.34, and 8.66, versus 0.94, 23.42, and 7.38 for 1D-AlexNet-OC. For 1D-LeNet-pH, the values were 0.89, 0.45, and 4.12, compared to 0.83, 0.57, and 3.07 for 1D-AlexNet-pH. These metrics, averaged over 10 runs, underscore the superior performance of the 1D-LeNet architecture in soil component prediction, with its high R^2 values indicating strong correlation between predictions and actual measurements.

http://www.aloki.hu ● ISSN 1589 1623 (Print) ● ISSN 1785 0037 (Online)
DOI: http://dx.doi.org/10.15666/aeer/2306_1073510749
© 2025, ALÖKI Kft., Budapest, Hungary

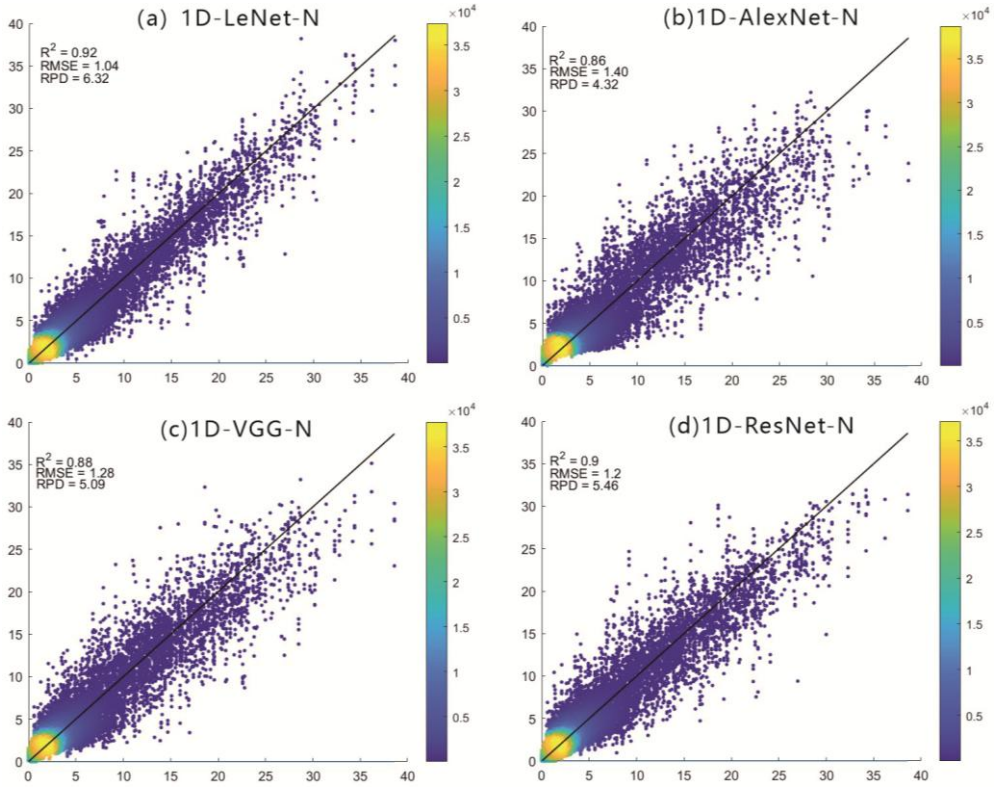

Figure 1. *Estimated vs. measured TN using 1D-CNN architectures over 10 test runs, with performance metrics*

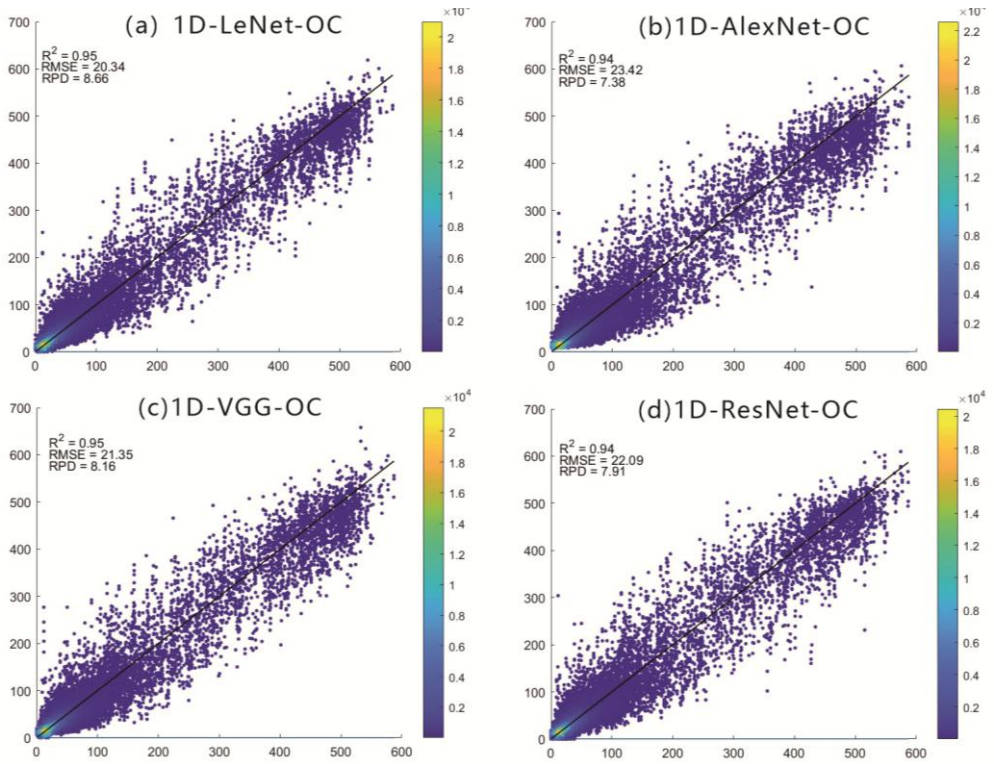

Figure 2. *Estimated vs. measured OC using 1D-CNN architectures over 10 test runs, with performance metrics*

http://www.aloki.hu ● ISSN 1589 1623 (Print) ● ISSN 1785 0037 (Online)
DOI: http://dx.doi.org/10.15666/aeer/2306_1073510749
© 2025, ALÖKI Kft., Budapest, Hungary

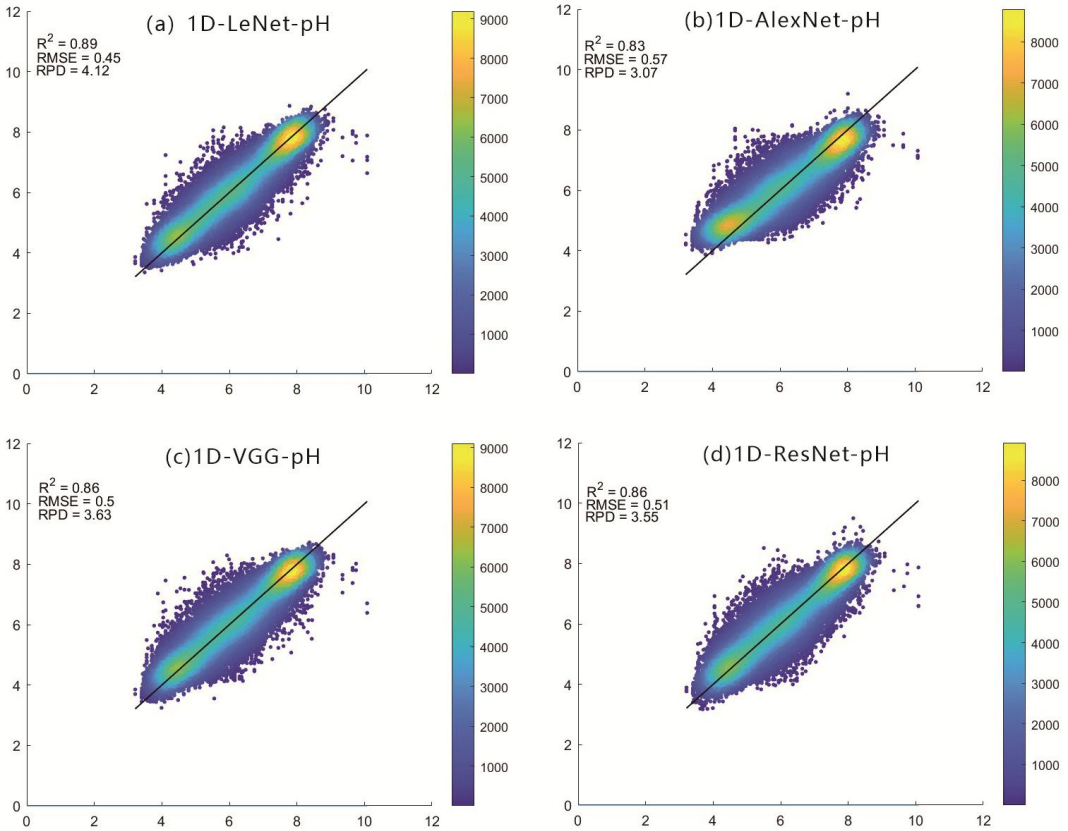

Figure 3. *Estimated vs. measured pH using 1D-CNN architectures over 10 test runs, with performance metrics*

Comparison of 1D-CNN, PLS, and SVM models

This study also applied PLS and SVM architectures to predict soil components TN, OC, and pH. *Figures 4–6* present scatter plots of observed vs. predicted values from 10 test runs, while *Figure 7* displays box plots of R^2 metrics from 1D-CNN, PLS, SVM approaches across the runs. The results demonstrate that all 1D-CNN models outperformed the SVM models in predicting the various soil components (*Fig. 7*). For instance, the average R^2 value for SVM-N was only 0.8, which was 12%, 6%, 8%, and 10% lower than the R^2 values of 1D-LeNet-N, 1D-AlexNet-N, 1D-VGG-N, and 1D-ResNet-N, respectively. Similarly, the average R^2 value for SVM-OC was 0.81, trailing 1D-LeNet-OC, 1D-AlexNet-OC, 1D-VGG-OC, and 1D-ResNet-OC by 14%, 13%, 14%, and 13%, respectively. For SVM-pH, the average R^2 value was 0.79, which was 10%, 4%, 7%, and 7% lower than the corresponding 1D-CNN models. Additionally, all 1D-CNN models, except for 1D-AlexNet-pH, also outperformed the PLS models (*Fig. 7*). The average R^2 value for PLS-N was 0.84, 8%, 2%, 4%, and 6% lower than 1D-LeNet-N, 1D-AlexNet-N, 1D-VGG-N, and 1D-ResNet-N, respectively. For PLS-OC, the average R^2 value was 0.89, which was 6%, 5%, 6%, and 5% lower than the respective 1D-CNN models. The average R^2 value for PLS-pH was 0.85, trailing 1D-LeNet-pH, 1D-VGG-pH, and 1D-ResNet-pH by 4%, 1%, and 1%, respectively. These findings suggest that deep learning models, particularly the 1D-CNNs, achieve superior performance over traditional models when applied to large datasets. *Table 2* summarizes the performance metrics for all models.

http://www.aloki.hu ● ISSN 1589 1623 (Print) ● ISSN 1785 0037 (Online)
DOI: http://dx.doi.org/10.15666/aeer/2306_1073510749
© 2025, ALÖKI Kft., Budapest, Hungary

Table 2. *Performance metrics of models for soil component prediction*

Model	Component	R^2	RMSE	RPD
1D-LeNet-N	TN	0.92	1.04	6.32
1D-AlexNet-N	TN	0.86	1.40	4.32
1D-VGG-N	TN	0.88	1.28	5.09
1D-ResNet-N	TN	0.90	1.20	5.46
PLS-N	TN	0.84	1.51	3.90
SVM-N	TN	0.80	1.65	4.33
1D-LeNet-OC	OC	0.95	20.34	8.66
1D-AlexNet- OC	OC	0.94	23.42	7.38
1D-VGG- OC	OC	0.95	21.35	8.16
1D-ResNet- OC	OC	0.94	22.09	7.91
PLS- OC	OC	0.89	29.66	4.91
SVM- OC	OC	0.81	40.19	4.91
1D-LeNet-pH	pH	0.89	0.45	4.12
1D-AlexNet-pH	pH	0.83	0.57	3.07
1D-VGG- pH	pH	0.86	0.50	3.63
1D-ResNet- pH	pH	0.86	0.51	3.55
PLS- pH	pH	0.85	0.53	3.28
SVM- pH	pH	0.79	0.61	2.80

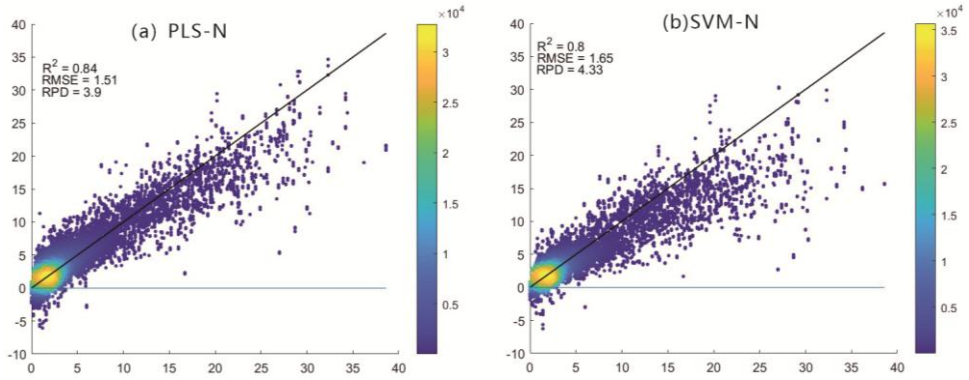

Figure 4. *Scatter plots of observed vs. predicted TN from 10 test runs for PLS and SVM models, with mean metrics shown*

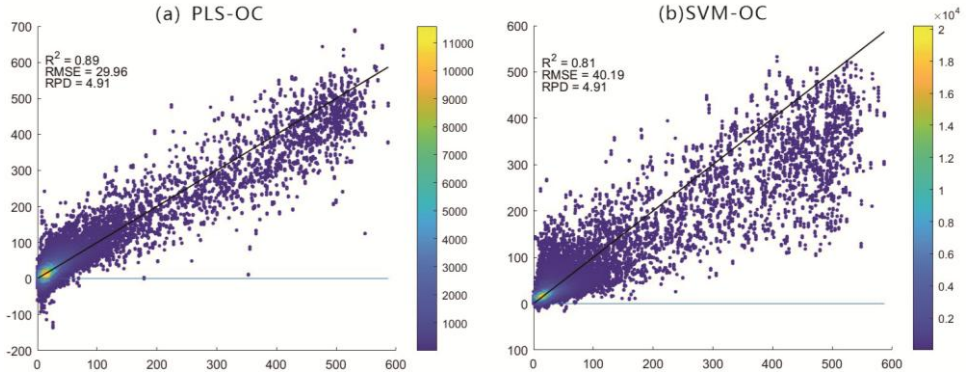

Figure 5. *Scatter plots of observed vs. predicted OC from 10 test runs for PLS and SVM models, with mean metrics shown*

http://www.aloki.hu ● ISSN 1589 1623 (Print) ● ISSN 1785 0037 (Online)
DOI: http://dx.doi.org/10.15666/aeer/2306_1073510749
© 2025, ALÖKI Kft., Budapest, Hungary

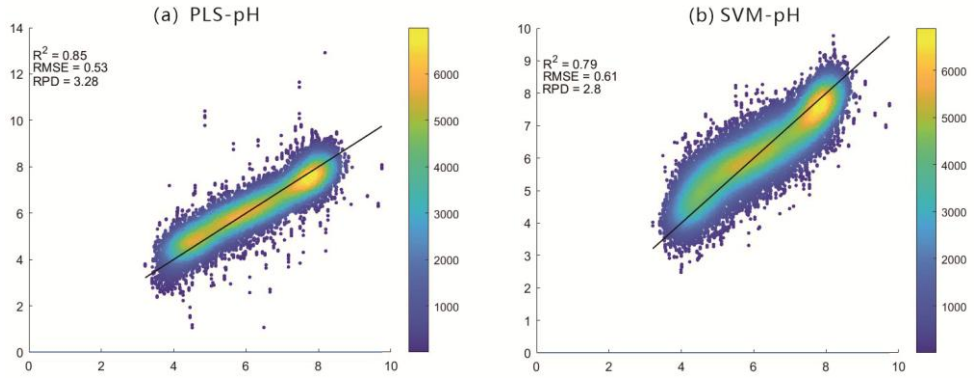

Figure 6. *Scatter plots of observed vs. predicted pH from 10 test runs for PLS and SVM models, with mean metrics shown*

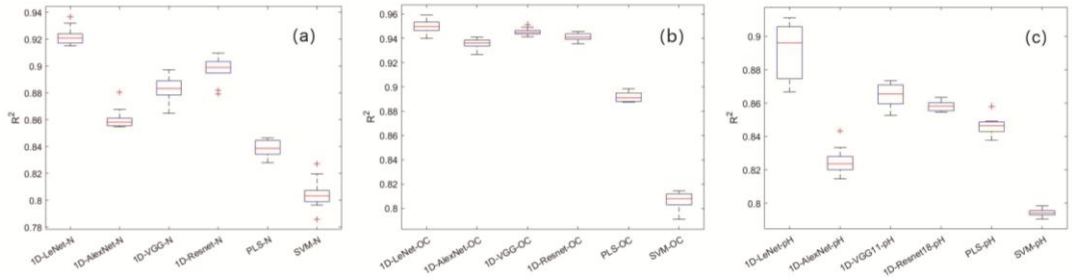

Figure 7. *Box plots of R² metrics from 10 test runs for 1D-CNN, PLS, SVM: (a) TN, (b) OC, (c) pH*

Feature band extraction in 1D-CNN models

To assess how each feature impacts the predictions made by 1D-CNN architectures, 100 samples were randomly drawn from the test dataset, and average absolute SHAP contributions were computed for each architecture. This approach helped pinpoint key wavelength bands that played prominent roles in model output generation. Additionally, we analyzed the correlation of log(R) with various soil components. The relative contribution of wavelengths in predicting soil TN, along with the correlation between log(R) and TN, is illustrated in *Figure 8*. Similar figures are provided for OC in *Figure 9* and pH in *Figure 10*.

The findings are as follows: (1) The average contribution of various wavelengths differed significantly across soil component predictions. Even within the same component, contributions varied between models. Specifically, for TN prediction: 1D-LeNet-N had notable contributions from the 2040–2050 nm range (*Fig. 8a*). 1D-AlexNet-N showed significant contributions from the 2470–2490 nm range (*Fig. 8b*). 1D-VGG-N had notable contributions from the 1410–1430 nm range (*Fig. 8c*).1D-ResNet-N showed strong contributions from wavelengths between 1580–1589 nm and 1640–1649 nm (*Fig. 8d*). 1D-AlexNet-OC showed strong contributions from wavelengths between 2200–2209 nm and 2120–2129 nm (*Fig. 9b*). 1D-VGG-OC had key contributions from wavelengths between 2190–2199 nm and 2140–2149 nm (*Fig. 9c*). 1D-ResNet-OC showed major contributions from wavelengths between 1230–1249 nm (*Fig. 9d*). For pH prediction: 1D-LeNet-pH contributions were significant from the 640–649 nm and 2100–

http://www.aloki.hu ● ISSN 1589 1623 (Print) ● ISSN 1785 0037 (Online)
DOI: http://dx.doi.org/10.15666/aeer/2306_1073510749
© 2025, ALÖKI Kft., Budapest, Hungary

2109 nm ranges (*Fig. 10a*). 1D-AlexNet-pH had strong contributions from wavelengths between 2040–2490 nm and 2140–2149 nm (*Fig. 10b*). 1D-VGG-pH showed major contributions from wavelengths between 2450–2459 nm and 2360-2369 nm (*Fig. 10*c). 1D-ResNet-pH had substantial contributions from wavelengths between 1080–1089 nm and 1100–1109 nm (*Fig. 10d*). (2) We found a negative correlation of log(R) with soil TN. Within wavelength regions showing stronger correlations (e.g., around 590 nm), the mean absolute SHAP values for all 1D-CNN-N models were relatively low (*Fig. 8*). This suggests that features with stronger negative correlations, despite their high absolute correlation, contributed less to the model predictions, indicating that the models may prioritize other features over those with strong negative correlations. A similar pattern was observed with soil OC (*Fig. 9*). A positive correlation was found between log(R) and soil pH. In wavelength regions with stronger correlations, such as around 600 nm, 1700 nm, and 2130 nm, the mean absolute SHAP values for all 1D-CNN-pH models were relatively high (*Fig. 10*). This indicates that these strongly positively correlated features played a larger role in the capability of the model to predict pH, implying that such features were more heavily relied upon for accurate predictions.

Discussion

Comparison of model performance

The study examined the efficacy of various 1D-CNN models, including 1D-LeNet, 1D-AlexNet, 1D-VGG, and 1D-ResNet, in predicting soil components (TN, OC, and pH) and compared their performance to traditional PLS and SVM models. The findings reveal that 1D-CNN models typically surpass traditional models in predictive accuracy. Notably, the shallow 1D-LeNet model consistently demonstrated superior performance across all components. Specifically, the average R^2 for 1D-LeNet-N is 0.92, which is 2%-4% higher than that of other 1D-CNN-N models, 8% higher than PLS-N, and 12% higher than SVM-N. The R^2 for 1D-LeNet-OC is 0.95, 1% higher than both 1D-AlexNet-OC and 1D-ResNet-OC, 6% higher than PLS-OC, and 14% higher than SVM-OC. The R^2 for 1D-LeNet-pH is 0.89, 3%-6% higher than other 1D-CNN-pH models, 4% higher than PLS-pH, and 10% higher than SVM-pH. These higher R^2 values suggest that shallow convolutional network architectures can more effectively capture important features in soil spectral data, thereby improving prediction accuracy. Several studies have confirmed the benefits of shallow 1D-CNN architectures for soil component prediction (Liu et al., 2023; Zhang et al., 2021). Moreover, comparisons with Tsakiridis et al. (2020) and Zhong et al. (2021) reinforce that shallow 1D-CNNs excel in spectral analysis, while our modified 1D-LeNet, optimized for large-scale soil datasets, achieves superior accuracy and efficiency. This enhanced performance supports precision agriculture by enabling rapid nutrient assessment.

Interpretability analysis

To further understand the internal mechanisms of 1D-CNN models, this study employed the SHAP method to explain model predictions. By calculating the average absolute SHAP values, the contribution of each wavelength to soil component prediction in 1D-CNN models was assessed. The SHAP values below the 1000 nm band are low for the TN and OC predictions, indicating that the contribution of visible light is not high towards the model predictions; instead, the model depends more on the near-infrared

http://www.aloki.hu ● ISSN 1589 1623 (Print) ● ISSN 1785 0037 (Online)
DOI: http://dx.doi.org/10.15666/aeer/2306_1073510749
© 2025, ALÖKI Kft., Budapest, Hungary

band. For instance, the models 1D-LeNet-N, 1D-AlexNet-N, 1D-AlexNet-OC, and 1D-VGG-OC are more dependent on bands beyond 2000 nm, whereas 1D-VGG-N, 1D-ResNet-N, and 1D-ResNet-OC are more dependent on bands at approximately 1500 nm; lastly, 1D-LeNet-OC depends upon bands centered at about 2000 nm and 1400 nm. However, for pH predictions, the 1D-LeNet-pH model exhibits high SHAP values at around 640 nm, indicating a significant contribution of visible light to pH predictions in this model. Similarly, like the 1D-AlexNet-pH and 1D-VGG-pH models, it also relies on wavelengths near 2000 nm, whereas the 1D-ResNet-pH model depends more on wavelengths around 1000 nm. Additionally, relative to other models, all 1D-LeNet models capture and utilize a broader spectrum of wavelength information, elucidating why the 1D-LeNet models outperform others.

The correlation between the log(R) and soil components varies across different wavelength bands. Specifically, log(R) demonstrates a negative correlation with both TN and OC, whereas it shows a positive correlation with pH. Bands characterized by strong negative correlations tend to contribute less to model predictions, whereas those with strong positive correlations significantly enhance predictive accuracy. For example, despite the strong negative correlation between log(R) and TN at the 590 nm band, this wavelength does not significantly influence predictions. Conversely, at the 600 nm, 1700 nm, and 2130 nm bands, where strong positive correlations exist between log(R) and pH, the larger SHAP values suggest these bands are crucial for pH predictions.

The SHAP analysis highlights key contributing wavelength bands (e.g., 2000 nm, 640 nm), which can guide the design of targeted spectral sensors. Further research into integrating mid-infrared methods could enhance predictions for nutrients like phosphorus (P) and potassium (K), which exhibit weak Vis-NIR responses.

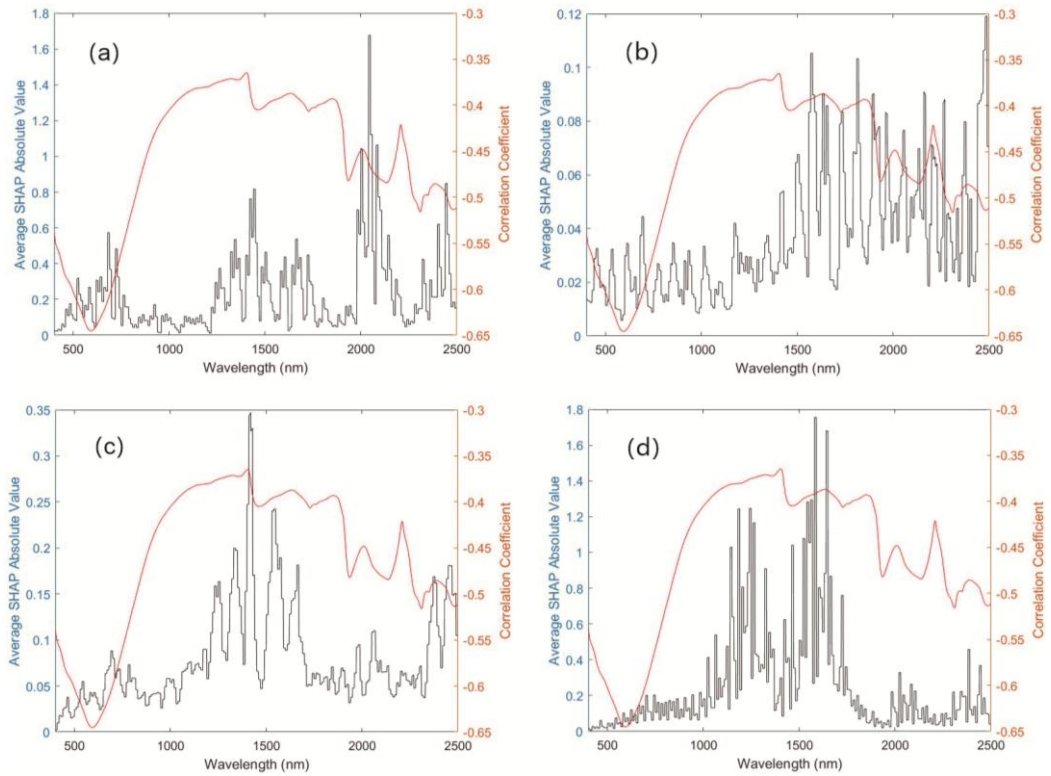

Figure 8. *Distribution of wavelength contributions (black curve) and correlation (red curve) for TN prediction models: (a) 1D-LeNet-N; (b)1D-AlexNet-N; (c) 1D-VGG-N; (d) 1D-ResNet-N*

http://www.aloki.hu ● ISSN 1589 1623 (Print) ● ISSN 1785 0037 (Online)
DOI: http://dx.doi.org/10.15666/aeer/2306_1073510749
© 2025, ALÖKI Kft., Budapest, Hungary

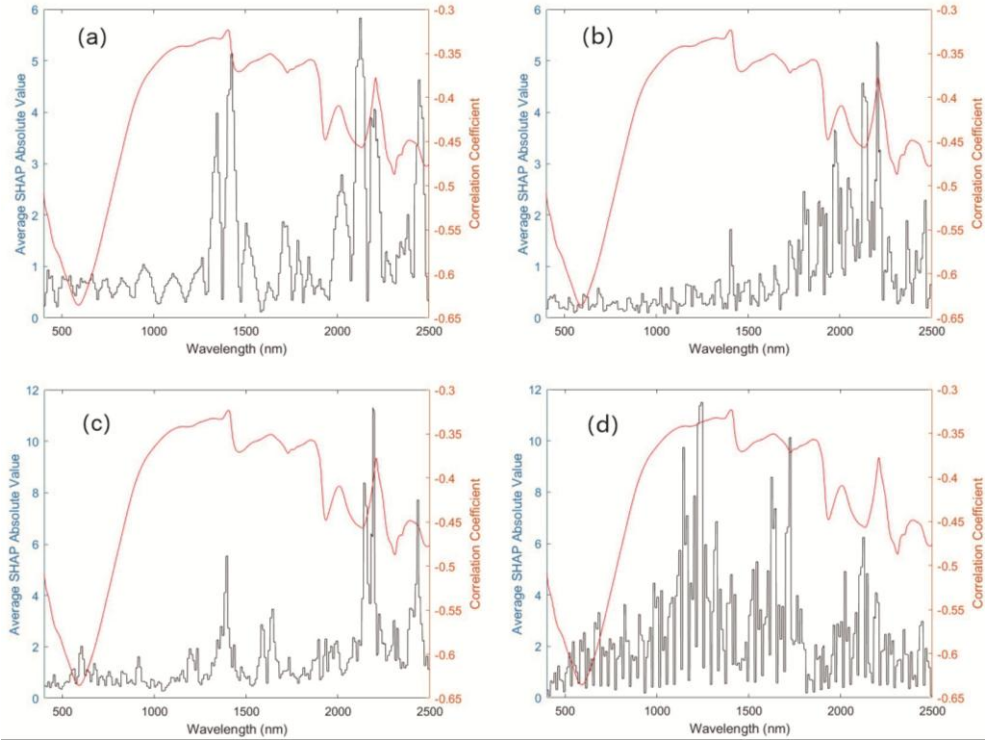

Figure 9. *Distribution of wavelength contributions (black curve) and correlation (red curve) for OC prediction models: (a) 1D-LeNet-OC; (b) 1D-AlexNet-OC; (c) 1D-VGG-OC; (d) 1D-ResNet-OC*

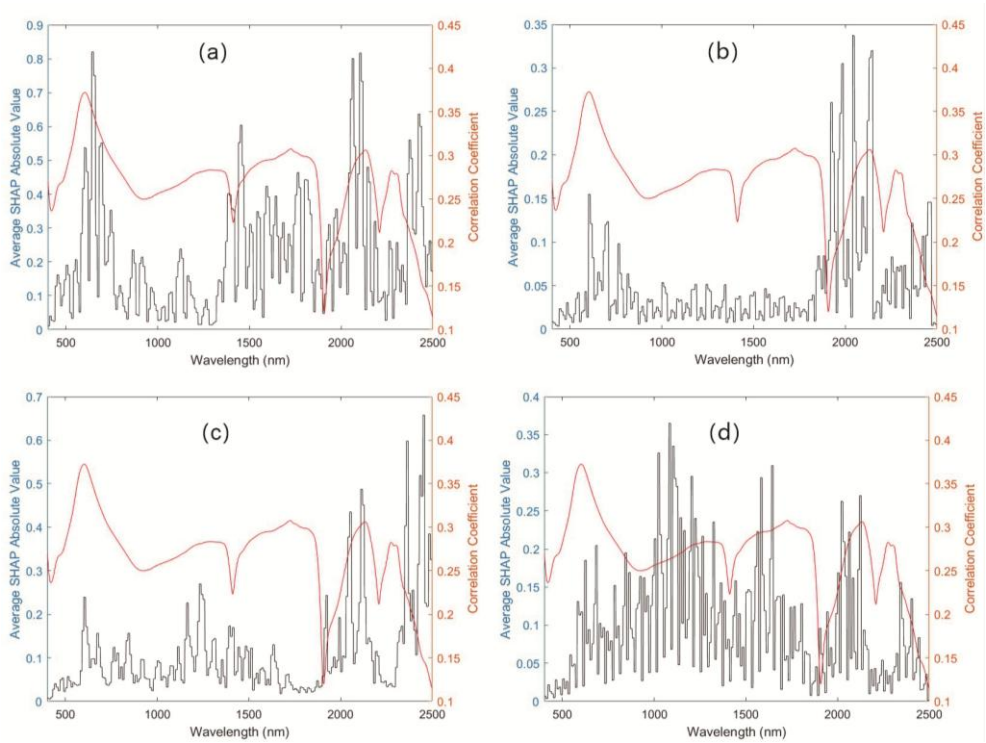

Figure 10. *Distribution of wavelength contributions (black curve) and correlation (red curve) for pH prediction models: (a) 1D-LeNet- pH; (b) 1D-AlexNet- pH; (c)1D-VGG- pH; (d) 1D-ResNet- pH*

http://www.aloki.hu ● ISSN 1589 1623 (Print) ● ISSN 1785 0037 (Online)
DOI: http://dx.doi.org/10.15666/aeer/2306_1073510749
© 2025, ALÖKI Kft., Budapest, Hungary

Conclusion

This study employed several 1D-CNN architectures, including 1D-LeNet, 1D-AlexNet, 1D-VGG, and 1D-ResNet, to predict soil components—namely, TN, OC, and pH. These models were evaluated against traditional methods like PLS and SVM. The main conclusions are as follows:

(1) 1D-CNN models significantly outperformed traditional methods regarding predictive performance, with 1D-LeNet exhibiting the strongest performance across all soil components. The R^2 values on the test set were 0.92 for TN, 0.95 for OC, and 0.89 for pH, underscoring the superior capability of shallow CNNs to extract and utilize features from soil spectral data.

(2) SHAP value analysis revealed how wavelength bands influenced predictions, elucidating their underlying prediction mechanisms. For example, the 1D-LeNet-N model demonstrated the greatest influence in TN prediction within the 2040-2050 nm band. Similarly, the 1D-LeNet-OC model was particularly effective in predicting OC within the 2120-2129 nm and 1420-1429 nm bands, while the 1D-LeNet-pH model was most predictive of pH in the 640-649 nm and 2100-2109 nm bands. These results highlight the considerable variation in how 1D-CNN architectures capture features of soil components, validating their effectiveness and scalability. Furthermore, they provide valuable insights for selecting spectral bands in future satellite sensors, which could enhance their design and improve soil component prediction.

Acknowledgments. The research was supported by the International Research Centre of Big Data for Sustainable Development Goals (CBAS) [Grant No. CBASYX0906], the National Natural Science Foundation of China (42271422) and the key project of sustainable development international cooperation program by NSFC (Grant No.42361144883), the Engineering Center of Yunnan Education Department for Health Geological Survey & Evaluation (9135009009), Science and Technology Innovation Team for Highland Ecological Agriculture Geological Survey and Evaluation of Yunnan Education Department.

REFERENCES

[1] Albinet, F., Peng, Y., Eguchi, T., Smolders, E., Dercon, G. (2022): Prediction of exchangeable potassium in soil through mid-infrared spectroscopy and deep learning: from prediction to explainability. – Artificial Intelligence in Agriculture 6: 230-241.

[2] Allo, M., Todoroff, P., Jameux, M., Stern, M., Albrecht, A. (2020): Prediction of tropical volcanic soil organic carbon stocks by visible-near- and mid-infrared spectroscopy. – Catena 189: 104452.

[3] Chen, S., Arrouays, D., Mulder, V. L., Poggio, L., Minasny, B., Roudier, P., Libohova, Z., Lagacherie, P., Shi, Z., Hannam, J. (2022). Digital mapping of GlobalSoilMap soil properties at a broad scale: a review. – Geoderma 409: 115567.

[4] Gruszczyński, S., Gruszczyński, W. (2022): Supporting soil and land assessment with machine learning models using the Vis-NIR spectral response. – Geoderma 405: 115451.

[5] He, K., Zhang, X., Ren, S., Sun, J. (2016): Deep residual learning for image recognition. – In: IEEE Conference on Computer Vision and Pattern Recognition, pp. 770-778.

[6] Huang, B., Sun, W., Zhao, Y., Zhu, J., Yang, R., Zou, Z., Ding, F., Su, J. (2007): Temporal and spatial variability of soil organic matter and total nitrogen in an agricultural ecosystem as affected by farming practices. – Geoderma 139(3-4): 336-345.

[7] Islam, K., Singh, B., Mcbratney, A. (2003): Simultaneous estimation of several soil properties by ultra-violet, visible, and near-infrared reflectance spectroscopy. – Soil Research 41: 1101-1114.

http://www.aloki.hu ● ISSN 1589 1623 (Print) ● ISSN 1785 0037 (Online)
DOI: http://dx.doi.org/10.15666/aeer/2306_1073510749
© 2025, ALÖKI Kft., Budapest, Hungary

[8] Kawamura, K., Nishigaki, T., Andriamananjara, A., Rakotonindrina, H., Tsujimoto, Y., Moritsuka, N., Rabenarivo, M., Razafimbelo, T. (2021): Using a one-dimensional convolutional neural network on visible and near-infrared spectroscopy to improve soil phosphorus prediction in Madagascar. – Remote Sensing 13(8): 1519.
[9] Ke, Z., Ren, S., Yin, L. (2024): Advancing soil property prediction with encoder-decoder structures integrating traditional deep learning methods in Vis-NIR spectroscopy. – Geoderma 449: 117006.
[10] Kok, Z. H., Mohamed Shariff, A. R., Alfatni, M. S. M., Khairunniza-Bejo, S. (2021): Support vector machine in precision agriculture: a review. – Computers and Electronics in Agriculture 191: 106546.
[11] Krichen, M. (2023): Convolutional neural networks: a survey. – Computers 12: 151.
[12] Krizhevsky, A., Sutskever, I., Hinton, G. (2012): ImageNet classification with deep convolutional neural networks. – Advances in Neural Information Processing Systems 60: 84-90.
[13] Lecun, Y., Bottou, L., Bengio, Y., Haffner, P. (1998): Gradient-based learning applied to document recognition. – Proceedings of the IEEE 86: 2278-2324.
[14] Liu, Y., Lu, Y., Chen, D., Zheng, W., Ma, Y., Pan, X. (2023): Simultaneous estimation of multiple soil properties under moist conditions using fractional-order derivative of vis-NIR spectra and deep learning. – Geoderma 438: 116653.
[15] Marcos Rafael, N., Demattê, J. A. M. (2006): Spectral reflectance methodology in comparison to traditional soil analysis. – Soil Science Society of America Journal 70: 393-407.
[16] Meng, X., Bao, Y., Luo, C., Zhang, X., Liu, H. (2024): SOC content of global Mollisols at a 30 m spatial resolution from 1984 to 2021 generated by the novel ML-CNN prediction model. – Remote Sensing of Environment 300: 113911.
[17] Omondiagbe, O. P., Roudier, P., Lilburne, L., Ma, Y., McNeill, S. (2024): Quantifying uncertainty in the prediction of soil properties using mid-infrared spectra. – Geoderma 448: 116954.
[18] Orgiazzi, A., Ballabio, C., Panagos, P., Jones, A., Fernández-Ugalde, O. (2017): LUCAS Soil, the largest expandable soil dataset for Europe: a review. – European Journal of Soil Science 69: 140-153.
[19] Piccoli, F., Rossini, M., Colombo, R., Schettini, R., Napoletano, P. (2023): A deep scalable neural architecture for soil properties estimation from spectral information. – Computers & Geosciences 180: 105433.
[20] Rinnan, Å., Berg, F. v. d., Engelsen, S. B. (2009): Review of the most common pre-processing techniques for near-infrared spectra. – TrAC Trends in Analytical Chemistry 28: 1201-1222.
[21] Seema, Ghosh, A. K., Das, B. S., Reddy, N. (2020): Application of VIS-NIR spectroscopy for estimation of soil organic carbon using different spectral preprocessing techniques and multivariate methods in the middle Indo-Gangetic plains of India. – Geoderma Regional 23: e00349.
[22] Shen, Z., Ramirez-Lopez, L., Behrens, T., Cui, L., Zhang, M., Walden, L., Wetterlind, J., Shi, Z., Sudduth, K. A., Baumann, P., Song, Y., Catambay, K., Viscarra Rossel, R. A. (2022): Deep transfer learning of global spectra for local soil carbon monitoring. – ISPRS Journal of Photogrammetry and Remote Sensing 188: 190-200.
[23] Stevens, A., Nocita, M., Tóth, G., Montanarella, L., van Wesemael, B. (2013): Prediction of soil organic carbon at the European scale by visible and near infrared reflectance spectroscopy. – PLoS ONE 8: e66409.
[24] Tsakiridis, N. L., Keramaris, K. D., Theocharis, J. B., Zalidis, G. C. (2020): Simultaneous prediction of soil properties from VNIR-SWIR spectra using a localized multi-channel 1-D convolutional neural network. – Geoderma 367: 114208.

http://www.aloki.hu ● ISSN 1589 1623 (Print) ● ISSN 1785 0037 (Online)
DOI: http://dx.doi.org/10.15666/aeer/2306_1073510749
© 2025, ALÖKI Kft., Budapest, Hungary

[25] Tsimpouris, E., Tsakiridis, N. L., Theocharis, J. B. (2021): Using autoencoders to compress soil VNIR–SWIR spectra for more robust prediction of soil properties. – Geoderma 393: 114967.
[26] Wu, Y., Chen, J., Wu, X., Tian, Q., Ji, J., Qin, Z. (2005): Possibilities of reflectance spectroscopy for the assessment of contaminant elements in suburban soils. – Applied Geochemistry 20: 1051-1059.
[27] Yang, J., Wang, X., Wang, R., Wang, H. (2020): Combination of convolutional neural networks and recurrent neural networks for predicting soil properties using Vis–NIR spectroscopy. – Geoderma 380: 114616.
[28] Zhang, Z., Ding, J., Zhu, C., Wang, J., Ma, G., Ge, X., Li, Z., Han, L. (2021): Strategies for the efficient estimation of soil organic matter in salt-affected soils through Vis-NIR spectroscopy: optimal band combination algorithm and spectral degradation. – Geoderma 382: 114729.
[29] Zhong, L., Guo, X., Xu, Z., Ding, M. (2021): Soil properties: their prediction and feature extraction from the LUCAS spectral library using deep convolutional neural networks. – Geoderma 402: 115366.
[30] Zhong, L., Guo, X., Ding, M., Ye, Y., Jiang, Y., Zhu, Q., Li, J. (2024): SHAP values accurately explain the difference in modeling accuracy of convolution neural network between soil full-spectrum and feature-spectrum. – Computers and Electronics in Agriculture 217.

http://www.aloki.hu ● ISSN 1589 1623 (Print) ● ISSN 1785 0037 (Online)
DOI: http://dx.doi.org/10.15666/aeer/2306_1073510749
© 2025, ALÖKI Kft., Budapest, Hungary